

# The Trinuclear Gallium-Bridged Ferrocenophane $[\{\text{Fe}(\eta^5\text{-C}_5\text{H}_4)_2\}_3\text{Ga}_2]$ : Synthesis, Bonding, Structure, and Coordination Chemistry

Alexander Althoff, Dirk Eisner, Peter Jutzi,\* Norman Lenze, Beate Neumann, Wolfgang W. Schoeller, and Hans-Georg Stammler<sup>[a]</sup>

**Abstract:** The trinuclear ferrocenophane  $[\{\text{Fe}(\eta^5\text{-C}_5\text{H}_4)_2\}_3\text{Ga}_2]$  (**3**) featuring two  $\text{sp}^2$ -hybridized gallium atoms in bridging positions between three ferrocene-1,1'-diyl units represents a novel type of ferrocene derivative. Compound **3** is obtained by thermal treatment of 1,1'-bis(dimethylgallyl)ferrocene (**1**) in nondonor solvents or in diethyl ether as solvent and subsequent thermal decomplexation. The [1.1]ferrocenophane  $[\{\text{Fe}(\eta^5\text{-C}_5\text{H}_4)_2\}\{\text{GaMe}_2\}_2]$  (**2**) is an intermediate in the formation of **3**. The reaction of **3** with an excess of trimethylgallium leads back to **1** and proves the reversibility of the multistep reaction sequence. Theoretical calculations reveal a carousel-type  $D_{3h}$  structure for **3**. The compound can best be

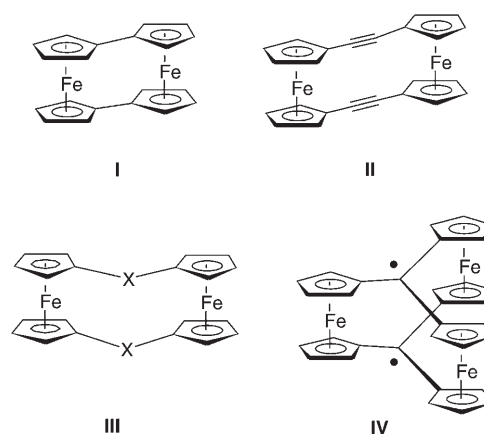
described as being composed of three only weakly interacting ferrocenediyl units covalently connected by gallium atoms without any  $\pi$ -bond contribution in the Ga–C bonds. Owing to steric constraints **3** cannot be reduced to the dianion  $\mathbf{3}^{2-}$ , which would feature a Ga–Ga bond. Compound **3** represents a stereochemically rigid difunctional Lewis acid allowing the formation of the adducts **3a–3d** possessing linear donor-acceptor-acceptor-donor arrangements. Crystal structure data for **3a–3d**

show a symmetry-reduced chiral ferrocenophane core ( $D_{3h} \rightarrow D_3$ ). A polymeric rodlike structure is observed for **3b** and **3d** caused by  $\pi$ -stacking effects (**3b**) or by a difunctional donor-acceptor interaction (**3d**). In solution, the chirality of the adducts is lost by rapid interconversion of the enantiomers. A cyclic voltammogram of **3b** in pyridine reveals three quasi-reversible oxidation steps at  $-356$ ,  $-154$ , and  $8$  mV, indicating only weak electron delocalization in the cationic species. The redox potentials of the pyridine adduct **3b** are compared with those of other pyridine-stabilized gallyl-substituted ferrocene derivatives and with ferrocene itself.

**Keywords:** dynamic covalent chemistry • electrochemistry • ELF (electron localization function) • metallocenes • organogallium compounds

## Introduction

One of the rich areas of metallocene chemistry is that of ferrocenophanes. Particularly interesting are those compounds in which the ferrocene units are fixed in a mutually coplanar geometry. This criterion is met ideally by the binuclear [m.m]ferrocenophanes [0.0]ferrocenophane  $[\{\text{Fe}(\text{C}_5\text{H}_4)_2\}_2]$  (**I**) and [2.2]ferrocenophane-1,13-diyne  $[\{\text{Fe}(\text{C}_5\text{H}_4)_2\}_2(\text{C}\equiv\text{C})_2]$  (**II**), and to a lesser extent by the [1.1]ferrocenophanes  $[\{\text{Fe}(\text{C}_5\text{H}_4)_2\}_2\text{X}_2]$  (**III**) ( $\text{X}=\text{CR}_2$ ).<sup>[1,2]</sup> Only a few heteroatom-



bridged compounds **III** ( $\text{X}=\text{BMe}_2^-$ ,  $\text{GaMe}$ ,  $\text{GaCH}(\text{SiMe}_3)_2$ ,  $\text{SiMe}_2$ ,  $\text{SnBu}_2$ ,  $\text{PbPh}_2$ ,  $\text{PMen}$ ;  $\text{Men}$  = menthyl) have been reported. They contain Group 13, 14, or 15 atoms in 1 and 12 position.<sup>[3]</sup> The existence of the carousel-like diradical  $[\{\text{Fe}$

[a] Dr. A. Althoff, D. Eisner, Prof. Dr. P. Jutzi, Dr. N. Lenze, B. Neumann, Prof. Dr. W. W. Schoeller, Dr. H.-G. Stammler  
Fakultät für Chemie  
Universität Bielefeld  
33615 Bielefeld (Germany)  
Fax: (+49) 521-106-6026  
E-mail: peter.jutzi@uni-bielefeld.de

Supporting information for this article is available on the WWW under <http://www.chemurj.org/> or from the author.

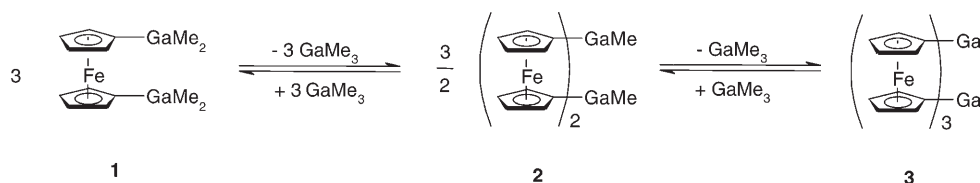
(C<sub>5</sub>H<sub>4</sub>)<sub>2</sub>]<sub>3</sub>C<sub>2</sub>] (**IV**), which is based on the tri(cyclopentadienyl)methyl system has been postulated as an interesting target molecule but was never prepared.<sup>[2]</sup> Traces of the trinuclear iron sandwich complex [Td<sub>2</sub>Fe<sub>3</sub>], which is based on the triindene trianion (Td), have been detected by mass spectrometry.<sup>[4]</sup>

Herein, we will describe the synthesis, characterization, and some chemistry of the trinuclear gallium-bridged ferrocenophane [[Fe(C<sub>5</sub>H<sub>4</sub>)<sub>2</sub>]<sub>3</sub>Ga<sub>2</sub>] (**3**) in which three ferrocene-1,1'-diyl units are held together by gallium atoms.

## Results

**Synthesis and structure of 3:** The trinuclear ferrocenophane [[Fe(C<sub>5</sub>H<sub>4</sub>)<sub>2</sub>]<sub>3</sub>Ga<sub>2</sub>] (**3**) was prepared from **1** or **2** under concomitant formation of trimethylgallium by several slightly different pathways. In the first variant **3** was prepared from a suspension of 1,1'-bis(dimethylgallyl)ferrocene (**1**)<sup>[5]</sup> in *p*-xylene under elimination of trimethylgallium at 150°C. In a second variant **3** was prepared by using the [1.1]ferrocenophane [[Fe(η<sup>5</sup>-C<sub>5</sub>H<sub>4</sub>)<sub>2</sub>]<sub>2</sub>[GaMe<sub>2</sub>]<sub>2</sub>] (**2**)<sup>[3b]</sup> as a starting material (Scheme 1). Third, **3** was formed by a solid-state decomposition of **1** or **2** at 200°C in vacuo. The same reaction sequence has been observed in the mass spectrometer: The condensation product **3**<sup>+</sup> was detected in the mass spectrum of **1** and **2**, the **1**<sup>+</sup> and **2**<sup>+</sup> peaks were not observed. In a fourth variant, **3** was prepared via the diethyl ether adduct **3a** (vide infra), which was formed from **1** in toluene/diethyl ether solution under concomitant formation of the diethyl ether adduct of trimethylgallium (see Scheme 3). This reaction took place when a solution of **1** in a mixture of toluene and diethyl ether was heated to 130°C in a closed flask. When dried in vacuo **3a** decomposed to give **3** in the form of an amorphous orange powder. Compound **3** is rather air sensitive and sparingly soluble in nondonor solvents. It has been characterized by NMR spectroscopy, EI mass spectrometry, and elemental analysis. The NMR spectrum was recorded in [D<sub>6</sub>]DMSO; it is evident that the spectrum shows data for the DMSO adduct **3c**. Experiments for the crystallization of base-free **3** have failed so far.

In a series of experiments we could show that the reaction sequence from **1** via **2** to **3** is fully reversible (Scheme 1). Compound **3** reacts in a closed flask at 100°C with a small excess of trimethylgallium under formation of **2** and with a larger excess under formation of **1**. In an earlier publication we already reported that **2** reacts with excess trimethylgallium under similar conditions to give **1**.<sup>[3b]</sup>



Scheme 1. Formation of **3**.

Quantum-chemical calculations carried out for **3** at the B3LYP/6-31G(d) level of theory led to the molecular structure shown in Figure 1.<sup>[6]</sup> Table 1 summarizes selected calcu-

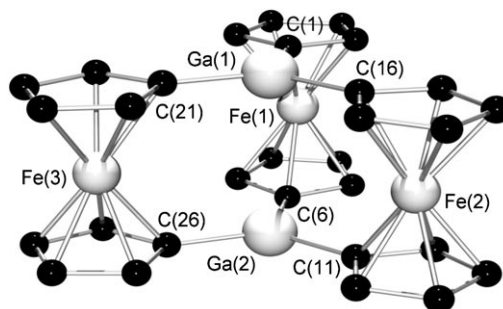


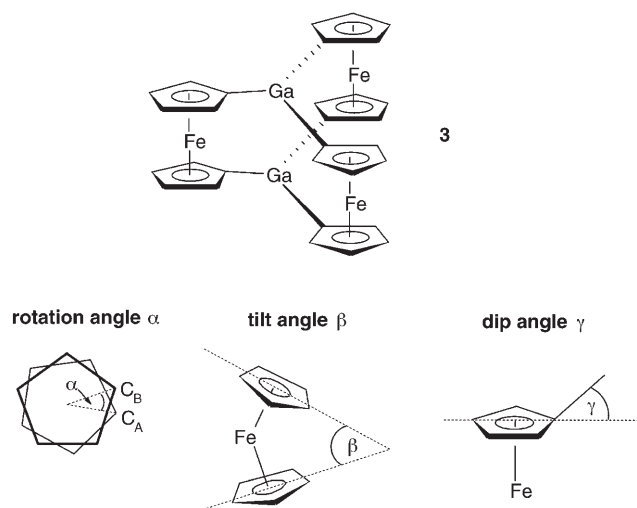
Figure 1. Molecular structure and numbering scheme of **3** as calculated at the B3LYP/6-31G(d) level of theory.

Table 1. Calculated(B3LYP/6-31G(d)) geometry parameters for **3**.

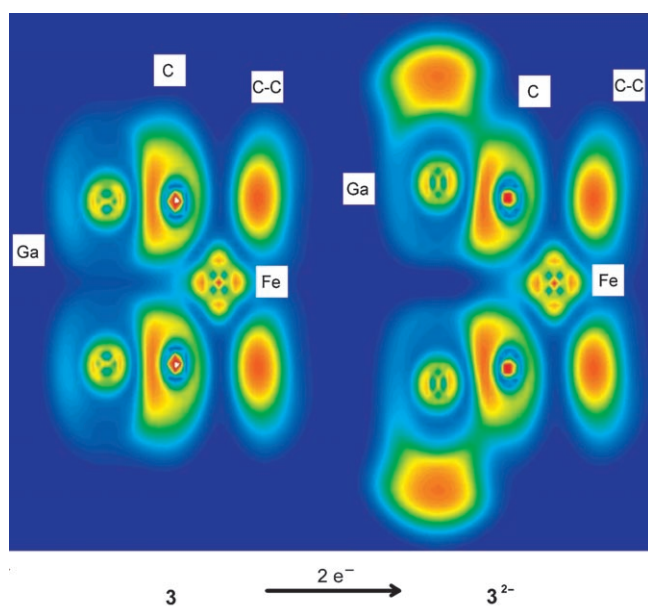
Distances [Å]		Angles [°]	
Ga(1)–C(1)	1.95	C(1)–Ga(1)–C(6A)	120
Ga(1)–C(16)	1.95	C(1)–Ga(1)–C(11)	120
Ga(1)–C(21)	1.95	C(6 A)–Ga(1)–C(11)	120
Fe(1)–Fe(2)	5.47	Cp–Cp rotation ( $\alpha$ )	0
Fe(1)–Fe(3)	5.47	Cp–Cp tilt ( $\beta$ )	3
Fe(2)–Fe(3)	5.47	dip angle ( $\gamma$ )	0
Ga–Ga	3.38	$\Sigma$ C–Ga–C	360

lated distances and angles. The structure of **3** shows that three ferrocene-1,1'-diyl units are linked together by two gallium(III) centers to form a *D*<sub>3h</sub> structure. The Ga–Ga separation is 3.38 Å, which is shorter than twice the van der Waals radius of gallium (1.87 Å<sup>[7]</sup>); the nonbonding distance between the Fe centers is 5.47 Å. Both gallium atoms have a trigonal-planar coordination geometry (C–Ga–C angle sum: 360°; C–Ga–C angles: 120°; Ga–C bonds: 1.95 Å). The six cyclopentadienyl ligands of the three ferrocene-1,1'-diyl units are arranged in an eclipsed, almost coplanar manner. The main structural features are given by the rotation ( $\alpha$ ), the tilt ( $\beta$ ) and the dip angle ( $\gamma$ ) (Figure 2). The parameters for **3** are  $\alpha = 0^\circ$ ,  $\beta = 3^\circ$ , and  $\gamma = 0^\circ$  (av).

Owing to the short Ga–Ga separation in **3** and owing to the suitable geometric constellation for the gallium p orbitals to overlap the question arises whether there is a bonding interaction between the two gallium atoms. Different MO analyses based on the natural bond orbitals (NBO)<sup>[8]</sup> and the electron localization function (ELF)<sup>[9]</sup> of **3** clearly

Figure 2. Definition of structural parameters in **3**.

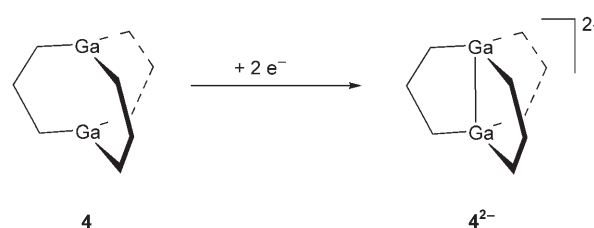
show no electron density in the center of the molecule, that is, between the two gallium atoms. The Wiberg bond order between the gallium atoms is 0.04. Thus, a bonding interaction along the Ga–Ga vector can be excluded. Another important conclusion must be drawn from the MO calculations: there is no  $\pi$ -electron density present in the (ferrocenediyl)carbon–gallium bonds. These results are illustrated in Figure 3 (left side) by an ELF representation of a Ga–Ga–Fe

Figure 3. ELF plots of **3** and **3**<sup>2-</sup>, showing the Ga–Ga–Fe plane. The electron pairs of the Ga–C bonds are polarized towards the C atoms due to the difference in electronegativity.

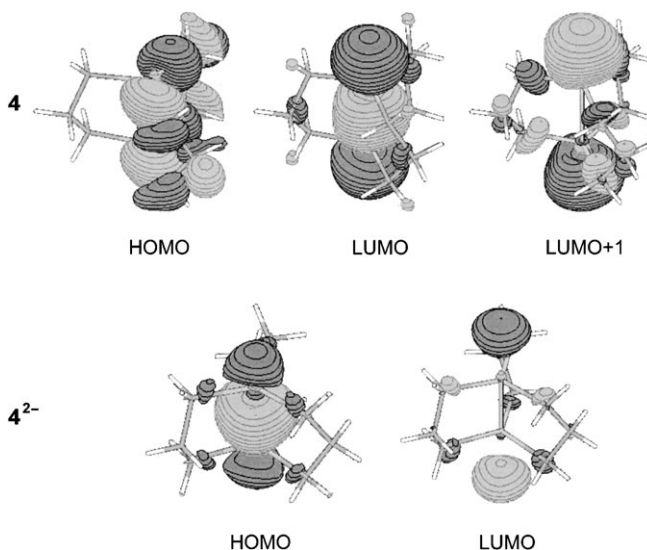
plane in **3** and by an MO picture of the HOMO in Figure 5. No essential  $\pi$ -electron delocalization from the ferrocenediyl units to the Ga atoms takes place and consequently no

electron density is available for a Ga–Ga interaction. The final bonding description of three electronically isolated ferrocene units held together by two gallium atoms is further substantiated by a comparison of the calculated Kohn–Sham orbitals of ferrocene and of **3**: The HOMO energies are identical for both systems (–5.2 eV).

One could expect that the reduction of **3** to **3**<sup>2-</sup> results in the formation of a Ga–Ga bond.<sup>[10]</sup> To prove the possibility of this type of Ga–Ga bond formation, an MO analysis has been performed on the model compound 1,5-digallabicyclo-[3.3.3]undecane (**4**), in which the three 1,1'-ferrocenediyl-groups of **3** have been substituted by  $-(\text{CH}_2)_3-$  spacers. The neutral compound **4** exhibits no Ga–Ga bonding interaction. However, strong bonding interactions are found in the dianion **4**<sup>2-</sup> (Scheme 2). The LUMO of **4** describes the bond-

Scheme 2. Reduction of **4**.

ing situation necessary to form the Ga–Ga bond. If two electrons are added to **4** the former LUMO becomes the new HOMO of the reduced species (Figure 4). Note that the Ga–Ga separation changes from 2.83 Å in the neutral compound to 2.36 Å in the dianion.

Figure 4. Molecular orbitals of **4** and **4**<sup>2-</sup>.

The possibility for a comparable two electron reduction of **3** to **3**<sup>2-</sup> under formation of a Ga–Ga bond has been investigated on the basis of theoretical calculations. The most im-

portant conclusions can be drawn from the molecular orbital pictures in Figure 5 and from the ELF plots in Figure 3. The LUMO of **3** describes the bonding situation necessary to

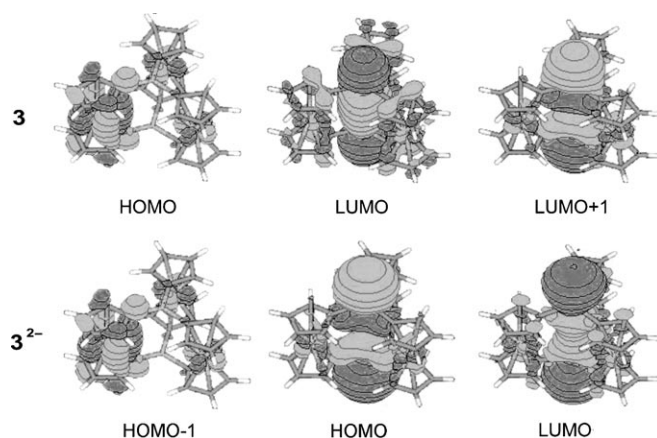
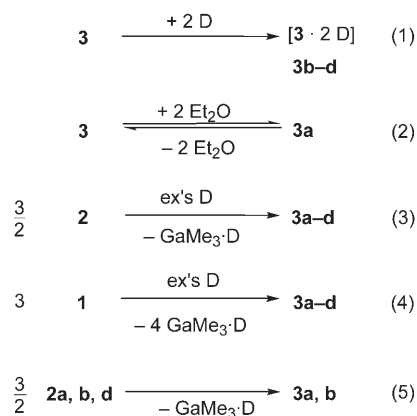


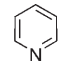
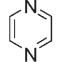
Figure 5. Molecular orbitals of **3** and **3<sup>2-</sup>**.

form a Ga–Ga bond. However, if two electrons are added they are not positioned in the LUMO but in the LUMO+1, which becomes the new HOMO, while the previous LUMO remains the LUMO of the reduced species **3<sup>2-</sup>**. The ELF analysis of **3<sup>2-</sup>** clearly shows that the two additional electrons are pointing *away* from the Ga–Ga center (see Figure 3, right side), which results in a pyramidalization at the Ga atoms and a lengthening of the Ga–Ga distance. An explanation for the lack of Ga–Ga bond formation is given by the fact that the Ga–Ga distance of **3** (3.38 Å) is much longer than a typical Ga–Ga  $\sigma$  bond (2.47–2.52 Å); a pronounced shortening of this distance is impossible due to the rigidity of the carousel-frame.

#### Synthesis and structure of coordination compounds **3a–d**:

The three-coordinate gallium atoms in **3** allow the formation of molecular and supramolecular coordination compounds.<sup>[3b,5]</sup> With monodentate donor molecules D, complexes of the type **3·2D** are formed; linear bidentate donors give rodlike polymeric complexes of the type **(3·D)<sub>∞</sub>**. The most straightforward method to synthesize such donor–acceptor complexes is the combination of the respective donor and acceptor molecules (Scheme 3, [Eq. (1)]). Compound **3a** (D=Et<sub>2</sub>O) is rather thermolabile and decomposes already at room temperature under formation of **3** and of diethyl ether (Scheme 3, [Eq. (2)]), complexes **3b** (D=pyridine), **3c** (D=DMSO) and **3d** (D=pyrazine) represent thermally stable compounds. The easy transformation of the ferrocenylgallane **1** into the ferrocenophane **2** and into the ferrocenophane **3** (Scheme 1) offers additional pathways for the formation of **3a–d** (Scheme 3, [Eq. (3) and (4)]). Thus, when **1** or **2** were dissolved in a mixture of toluene and the respective donor and were then warmed up to 130 °C in a closed flask until a clear solution had formed, the adducts **3a–d** could be isolated as X-ray quality crystals after cooling



	2a, 3a	2b, 3b	3c	2d, 3d
D	Et <sub>2</sub> O		DMSO	

Scheme 3. Formation of the adducts **3a–d**.

to room temperature. In the remaining solution, the donor adducts of trimethylgallium could be detected by NMR spectroscopy. Another variant started with a suspension of **2a**, **2b**, or **2d** in toluene. Heating to 150 °C resulted in the formation of **3a** or **3b** and of the respective donor adduct of trimethylgallium (Scheme 3, [Eq. (5)]). Utilizing the easy exchange of donor molecules, **3b** could also be prepared from the donor complexes **3a** or **3c** and excess pyridine at 130 °C. Similarly, the donor adduct **3c** was prepared by starting from complexes **3a** or **3b**. From a synthetic point of view the preparation of **3a–d** is most easily performed starting from **1** as the ferrocenylgallium component.

The compounds **3a–d** have been characterized by using X-ray crystal structure analysis, NMR spectroscopy, mass spectrometry, elemental analysis, cyclic voltammetry, and spectroelectrochemistry. They are only sparingly soluble in nondonor solvents. The solubility of **3a**, **3b**, and **3d** in DMSO stems from the formation of the adduct **3c**. The NMR spectra were recorded in [D<sub>6</sub>]DMSO; thus, the spectra show data for the DMSO adduct **3c** and for the free donor molecules. In the mass spectra of **3a–d** the peaks of the molecular ions [3·2D]<sup>+</sup> could not be detected; instead, the fragments **3<sup>+</sup>** and D<sup>+</sup> have been observed.

Drawings of the molecular structures of **3a–d** in form of a thermal ellipsoid plots are given in Figure 6 and Figure 7. Table 2 summarizes selected bond lengths and angles. The drawings of **3a–d** show that three ferrocene-1,1'-diyl units are linked together by two donor-stabilized gallium(III) centers to form the expected carousel structure. The pyramidalization of the gallium centers results in a deviation of the Cp(centroid)-C(Cp)-Ga units from linearity and in a distortion of the ferrocene-1,1'-diyl units. Owing to the pyramidalization of the gallium centers the Ga–Ga separation is

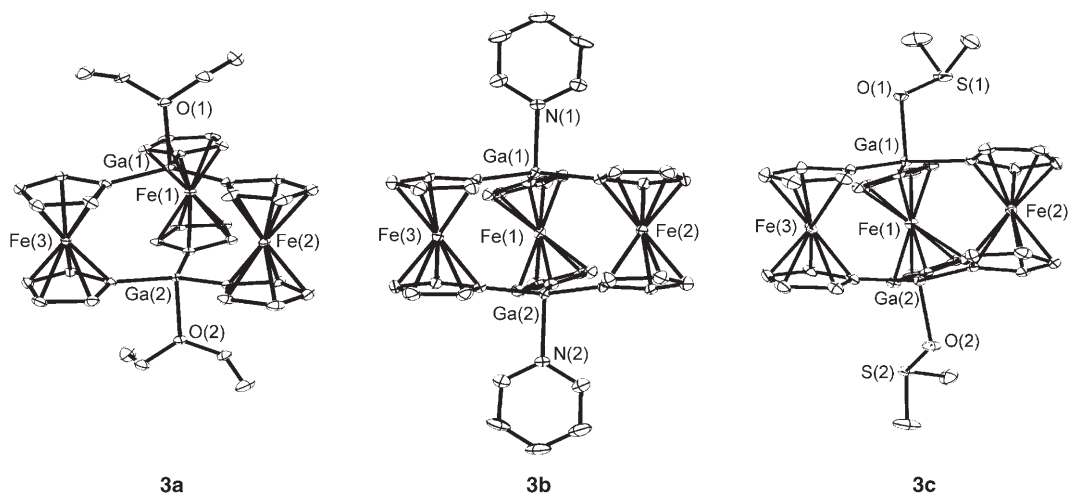


Figure 6. Molecular structures of **3a**, **3b**, and **3c** (thermal ellipsoids at 50% probability).

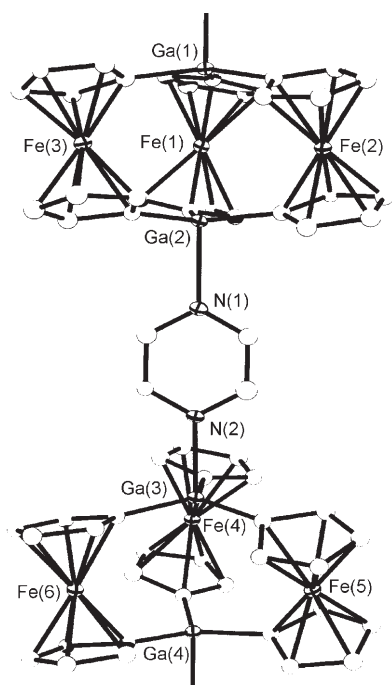


Figure 7. Part of the polymeric structure of **3d** (thermal ellipsoids at 50% probability).

greater than in **3**. The six cyclopentadienyl ligands of the three ferrocene-1,1'-diyl units deviate from a mutually coplanar arrangement in such a way that they are tilted relative to the Ga–Ga axis. The clockwise or counter-clockwise orientation gives rise to components having a slightly twisted and thus chiral structure. The rotation angles  $\alpha$  (see Figure 2) can be used to measure of the amount of twist.

The diethyl ether complex **3a** crystallizes in the monoclinic space group  $C2/c$ . The Ga–Ga separation is 3.72 Å which is roughly double the van der Waals radius of gallium (1.87 Å); the average nonbonding distance between the Fe centers is 5.49 Å. The gallium centers have a slightly distort-

ed trigonal-pyramidal coordination geometry (C–Ga–C angle sum: 357°; C–Ga–O angles: 97.84(6), 94.36(6), 93.67(6)°; Ga–C bonds: 1.9461(16), 1.9499(16), 1.9516(16) Å). The Ga–O bond lengths of 2.1551(12) Å are comparable to those of the digallaferrocenophane diethyl ether adduct **2a** (2.153(2) Å).<sup>[3b]</sup> The C(Cp)–Ga bonds, with reference to the Cp ring plane, are bent away from the iron centers by  $\gamma = 4^\circ$ . A slight deviation of the Cp ligands within the ferrocene-1,1'-diyl units from a mutually parallel arrangement is observed ( $\beta = 3^\circ$ ). The rotation angle  $\alpha$  is 5°.

The pyridine complex **3b** crystallizes as [**3b**·1.5 toluene] in the monoclinic space group  $C2/c$ .<sup>[11]</sup> It shows a disorder of toluene molecules. A drawing of the structure without the disordered toluene molecules is given in Figure 6. The ferrocenophane framework parameters are comparable to those of **3a**. The Ga–N bond lengths of 2.143(14) Å are similar to those of **2b** (2.144(5) Å).<sup>[3b]</sup> The angles in **3b** are  $\alpha = 11^\circ$ ,  $\beta = 4^\circ$ , and  $\gamma = 4^\circ$ . The C–Ga–C angle sum is 355°. Therefore, complex **3b** is more twisted (greater  $\alpha$ ) and more pyramidalized (lower C–Ga–C angle sum) than **3a**. A polymeric rodlike structure is observed for **3b** caused by  $\pi$ -stacking interactions between the pyridine molecules. The distance between the pyridine ring-planes is 3.45 Å.

The DMSO complex **3c** crystallizes as [**3c**·DMSO] in the orthorhombic space group  $Pbca$ . The crystals show a disorder of DMSO molecules at two positions. A drawing of the molecular unit of [**3c**·DMSO] is given in Figure 6. The DMSO molecules coordinate at the gallium atoms of **3** through their oxygen atoms. This corresponds well to the fact that oxygen donors are stronger Lewis bases with respect to Ga<sup>III</sup> centers than sulfur atoms.<sup>[12]</sup> The angles in **3c** are  $\alpha = 15^\circ$ ,  $\beta = 3^\circ$  and  $\gamma = 3^\circ$ . The C–Ga–C angle sum is 357°.

Depending on the preparation method the rodlike polymeric pyrazine complex **3d** crystallizes in different pseudopolymorphic modifications. Exemplary ferrocenophane framework parameters are given for one modification which crystallizes as [**3d**·0.75 toluene] in the triclinic space group  $P\bar{1}$ . It shows a disorder of toluene molecules. A drawing of a

Table 2. Selected distances [ $\text{\AA}$ ] and angles [ $^\circ$ ] for **3a-d**.

	<b>3a</b>	<b>3b</b> ·1.5 toluene	<b>3c</b> ·DMSO	<b>3d</b> ·0.75 toluene
distances				
Ga(1)–C(1)	1.9516(16)	1.968(19)	1.952(2)	1.963(4)
Ga(1)–C(16)	1.9461(16)	1.965(17)	1.958(2)	1.943(4)
Ga(1)–C(21)	1.9499(16)	1.973(17)	1.957(2)	1.961(4)
Ga(1)–N/O	2.1551(12)	2.143(14)	2.0984(13)	2.280(3)
Ga–Ga	3.72	3.87	3.80	3.81
Fe(1)–Fe(2)	5.45	5.40	5.47	5.46
Fe(1)–Fe(3)	5.45	5.40	5.36	5.41
Fe(2)–Fe(3)	5.51	5.58	5.48	5.38
angles				
C(1)–Ga(1)–C(16)	118.61(7)	117.9(8)	121.10(9)	120.43(15)
C(1)–Ga(1)–C(21)	118.85(7)	116.8(7)	117.34(9)	118.39(16)
C(16)–Ga(1)–C(21)	120.03(7)	120.6(8)	118.07(9)	117.35(15)
N/O–Ga(1)–C(1)	97.84(6)	98.1(7)	98.10(7)	93.87(12)
N/O–Ga(1)–C(16)	94.36(6)	95.0(6)	95.05(7)	97.33(12)
N/O–Ga(1)–C(21)	93.67(6)	98.8(7)	95.53(7)	98.45(12)
Cp–Cp rotation ( $\alpha$ )	5	11	15	14
Cp–Cp tilt ( $\beta$ )	4	4	3	4
dip angle ( $\gamma$ )	4	4	3	4
$\Sigma$ C–Ga–C	357	355	357	356

part of the structure without the disordered toluene molecules is given in Figure 7. The Ga–N bond lengths of 2.280(3)  $\text{\AA}$  are slightly longer than those of **2d** (2.1854(14)  $\text{\AA}$ ).<sup>[3b]</sup> The angles in **3d** are  $\alpha=14^\circ$ ,  $\beta=4^\circ$  and  $\gamma=4^\circ$ . The C–Ga–C angle sum is 356 $^\circ$ .

Recently we reported that the complex **2b** reacts with excess trimethylgallium under formation of **1** and the pyridine adduct of trimethylgallium.<sup>[3b]</sup> Similarly, the complexes **3a-c** react with excess trimethylgallium under formation of **1** or **2**, respectively, and the corresponding donor adducts of trimethylgallium. It is concluded from these experiments that the reversibility according to Scheme 1 can also be observed in systems containing the donor adducts of **1**, **2**, and **3**.

**Electrochemistry of 3b:** A cyclic voltammogram of **3b** was recorded by using pyridine as solvent and tetrabutylammonium fluoride (TBAPF) as the supporting electrolyte. Quasi-reversible oxidation potentials are observed at  $E_{1/2}(1)=-356$  mV,  $E_{1/2}(2)=-154$  mV, and  $E_{1/2}(3)=8$  mV (versus ferrocene/ferrocenium), with a peak separation of 90 mV (Figure 8). The differences in the oxidation potentials ( $\Delta E_{1/2}(2-1)=202$  mV (**3b**<sup>+</sup>/**3b**<sup>2+</sup>) and  $\Delta E_{1/2}(3-2)=162$  mV (**3b**<sup>2+</sup>/**3b**<sup>3+</sup>) indicate only a partial electron delocalization in the cationic species (presumably, class II in the Robin and Day classification<sup>[1]</sup>). The  $\Delta E_{1/2}(2-1)$  value is comparable to that observed for **2b**.<sup>[3b]</sup>

Oxidation of ferrocenophanes might result in changes of optical properties due to inter-valence charge-transfer interactions.<sup>[13]</sup> Spectroelectrochemical studies performed with solutions of **3b** have not shown any charge-transfer effect. The optical properties of **3b**<sup>+</sup>, **3b**<sup>2+</sup>, and **3b**<sup>3+</sup> are comparable to those of the parent ferrocene<sup>[14]</sup> and indicate the presence of nearly isolated ferrocenediyl units.

**Dynamic behavior of 3c in solution:** Both the <sup>1</sup>H and the <sup>13</sup>C NMR spectrum of **3c** display only one set of signals for

the  $\alpha$ -CH and one set for the  $\beta$ -CH units of the three ferrocene-1,1'-diyl fragments. This observation indicates an averaged, highly symmetrical structure in solution. It is assumed that there occurs a rapid interconversion of the enantiomers as well as a rapid motion of the donor molecules and of the ferrocenophane fragment around the Ga–Ga axis.

To analyze the interconversion of the enantiomers in more detail we have computed the model complex **3**·2NH<sub>3</sub> within  $D_{3h}$  and alternatively within  $D_3$  geometry. The latter

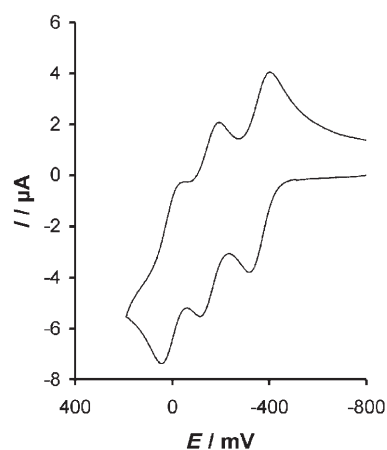


Figure 8. Cyclic voltammogram of a solution of **3c** in pyridine (0.1 M NBu<sub>4</sub>PF<sub>6</sub>).

refers to the N-donor-stabilized adducts **3c** and **3d**. A pictorial representation is summarized in Figure 9.

The calculated structures (RI-BP86/SV(P) level<sup>[15]</sup>) presume the following aspects: lowering the symmetry ( $D_{3h} \rightarrow D_3$ ) shrinks the N–Ga bond lengths and reduces the strain under formation of sp<sup>3</sup>-hybridized Ga centers. The energy profit due to symmetry lowering is rather small, and amounts to  $-2.7$  kcal mol<sup>-1</sup> (without zero-point energy correction). This gives credit to the belief that at room temperature the donor adduct **3c** and in general all complexes of **3** undergo strong tumbling, as documented by the effects measured in the solution-NMR spectra.

## Discussion

A novel route to [1.1]ferrocenophanes has been found with the synthesis of the gallium-bridged ferrocenophane [[Fe(C<sub>5</sub>H<sub>4</sub>)<sub>3</sub>]<sub>2</sub>Ga<sub>2</sub>] (**3**) and of its donor adducts **3a-d**. The syn-

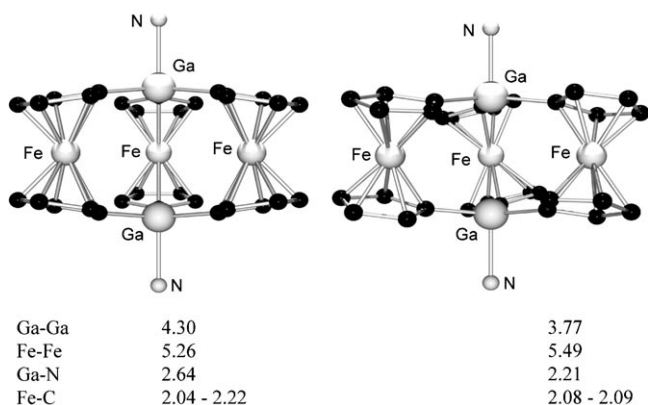
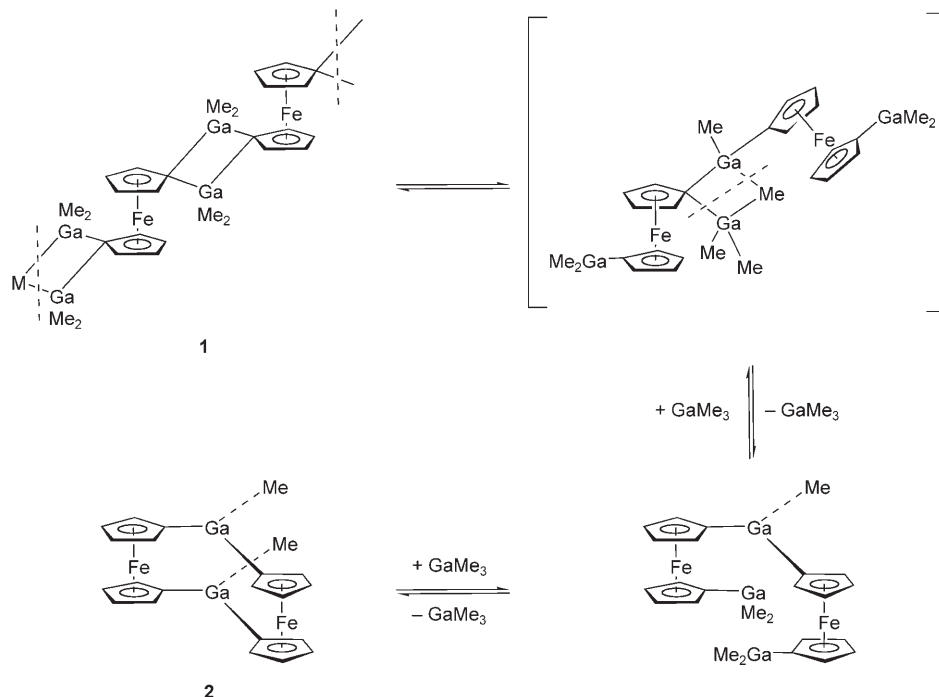


Figure 9. Plot of the equilibrium geometries of  $3 \cdot 2\text{NH}_3$  within  $D_{3h}$  (left) and  $D_3$  (right) geometries, calculated at RI-BP86/SV (P) level. Bond lengths are in Angströms, bond angles in degrees. Hydrogen atoms are omitted for clarity,  $\text{N}=\text{NH}_3$ .

thetic strategy depends on rather weak C(ferrocenyl)–gallium and C(methyl)–gallium bonds, so that substituent exchange reactions can take place easily. Thus, heating of  $[\text{Fe}(\text{C}_5\text{H}_4\text{GaMe}_2)_2]$  (**1**) leads under elimination of trimethylgallium in quantitative yields to the formation of **3** via the [1.1]ferrocenophane  $[\{\text{Fe}(\text{C}_5\text{H}_4)_2\}_2[\text{GaMe}_2]]$  (**2**). Donor adducts of **3** are formed under comparable conditions starting from donor adducts of **1**. Highly stereo- and regiospecific substitution reactions at the gallium atoms are necessary to transform **1** into **3**. A plausible reaction sequence for the formation of the stable intermediate **2** is shown in Scheme 4. The weakness of the Ga–C(ferrocenediyl) bridge bond and



Scheme 4. Postulated reaction sequence for the formation of **2**.

the chance for the formation of a bridging methyl group in a reactive intermediate or transition state are the prerequisite for the extrusion of trimethylgallium and the concomitant formation of a novel Ga–C(ferrocenediyl) bond.<sup>[16]</sup> The formation of **3** proceeds via intermediates resembling that shown in brackets in Scheme 4. Owing to the complexity of these transformations, reversibility of reaction sequences (proof-reading) seems to be necessary. Not surprisingly in this context, the ferrocenophane **3** can be transformed back to **1** in the presence of excess trimethylgallium at temperatures of about 100°C (see Scheme 1). Comparable activation barriers for the forward and the backward reactions, the large excess of one reactant (trimethylgallium) and/or the low solubility and easy crystallization of one of the products have been shown to be responsible for the selective product formation. These are criteria for reactions performed under the concept of “dynamic covalent chemistry”.<sup>[17]</sup>

Compound **3** is an example of a stereochemically rigid difunctional Lewis acid.<sup>[18]</sup> It is the first molecule containing two Lewis acidic main-group element centers fixed in a manner that allows Lewis bases to be bonded along a linear base-acid-acid-base vector. These geometric constraints result in a high synthetic potential for the formation of complexes such as **3b** and **3d**, which crystallize in the form of supramolecular rods. Further examples of such compounds will be presented in a forthcoming publication.

While the base-free **3** is an achiral compound, the coordination of donor molecules results in a left-hand or right-hand twist of the carousel structure and therefore in the formation of chiral species as shown by the presence of two enantiomers in the solid-state structures of **3a–d**. The

amount of twist can be measured by the rotation angles  $\alpha$ . The conformational isomerization of **3a–d** can be compared to the situation found in atropisomeric molecular propellers like in some triarylboranes.<sup>[19]</sup> The dynamic structure of adducts of **3** in solution is based on the fast interconversions of the observed enantiomers. The solid-state structures of **3a–d** will be discussed in detail in a forthcoming publication, together with the structures of further coordination compounds of **3**.

The electronic communication in multiferrocenyl systems has been studied already in great detail.<sup>[1]</sup> In general, the electronic coupling depends on the rigidity of the ferrocene-containing framework, on the distance between the iron centers, and on the degree of elec-

tron mobility in the respective bridging unit. In the class of ferrocenophanes (see Figure 1), the [0.0]ferrocenophane **1** is a strongly interacting system, whereas the [1.1]ferrocenophanes of type **II** are only weakly interacting.<sup>[1]</sup> Also compound **3b**, which is a type **IV** ferrocenophane with the two carbon bridges substituted by two pyridine-gallium units, represents a weakly interacting system. This is concluded from electrochemical and spectroelectric measurements, which are the most widely used tools to investigate the electronic communication.<sup>[14]</sup>

It is worth mentioning that the electronic behavior of **3b** differs from that observed for the pyridine adduct of triferrocenylgallium.<sup>[20]</sup> Whereas **3b** exhibits three separate oxidation steps in the cyclic voltammogram (see Figure 9 and Figure 10), the ferrocenyl units of triferrocenylgallium are oxidized simultaneously. This difference is attributed to the fact that all ferrocenyl groups of triferrocenylgallium are freely rotating and thus fully independent, while those of **3b** are fixed in a carousel-type structure and thus are capable of some weak electronic communication.

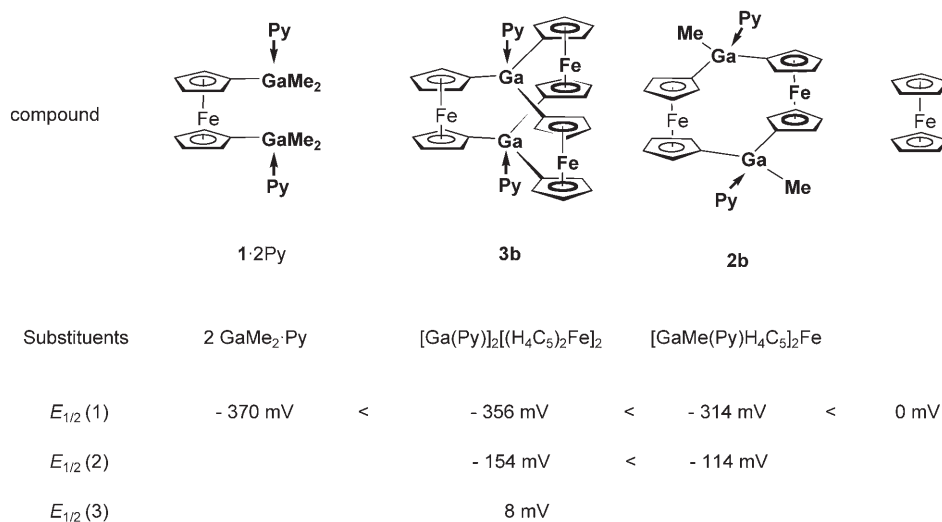


Figure 10. First oxidation potentials (in pyridine) of substituted ferrocenes (functional groups printed in bold letters). For **2b** and **3b** also the second (and third) oxidation potential is shown.

On the basis of the CV data for **3b** measured in the present work and of the CV data described in two earlier publications, the first oxidation potentials of ferrocene and of the so far known pyridine-gallium substituted ferrocene derivatives are compared (Figure 10). The ferrocene derivatives [Fe(C<sub>5</sub>H<sub>4</sub>GaMe<sub>2</sub>Py)<sub>2</sub>] (**1·2Py**),<sup>[5]</sup> [Fe({GaMe(Py)H<sub>4</sub>C<sub>5</sub>})<sub>2</sub>Fe] (**2b**),<sup>[3b]</sup> and [Fe({Ga(Py)H<sub>4</sub>C<sub>5</sub>})<sub>2</sub>Fe] (**3b**) are oxidized more easily than the parent ferrocene. The electron-donating ability decreases in the direction **1·2Py** > **3b** > **2b**. Thus, starting from the parent ferrocene as reference the substitution of hydrogen atoms for pyridine-stabilized diorganogallyl groups causes an easier oxidation of the ferrocene derivative. The easier oxidation of **3** compared with **2** still lacks a plausible explanation.

The ferrocenophane **3** is the first representative of a new class of compounds and offers several aspects for further detailed studies of the parent compound and of its derivatives.

From a synthetic point of view the preparation of a molecule representing a “molecular-level carousel” is challenging. In this context, the ferrocenophane **3** or a properly substituted derivative has to be fixed in a framework structure with the help of suitable donor centers. It is worth investigating whether the ferrocenophane-rotation within such a framework can be controlled by external stimuli.<sup>[21]</sup>

## Experimental Section

**General comments:** All manipulations were carried out under a purified argon atmosphere using standard Schlenk techniques. The solvents were commercially available, purified by conventional means, and distilled immediately prior to use. The NMR spectra were recorded in [D<sub>6</sub>]DMSO using a Bruker Advance DRX 500 spectrometer (<sup>1</sup>H 500.1 MHz; <sup>13</sup>C 125.8 MHz). Chemical shifts are reported in ppm and were referenced to the solvent resonances as internal standard. The mass spectra (EI) were

recorded on a VG Autospec mass spectrometer. Only characteristic fragments and isotopes of the highest abundance are listed. The elemental analyses were performed by the Microanalytical Laboratory of the Universität Bielefeld. The cyclic voltammogram was recorded on an EG&G potentiostat, Model 273A, controlled by M 250/270 software. The supporting electrolyte was tetrabutylammonium fluoride (TBAPF), which was purchased from Fluka and used without further purification. The electrolyte concentration was 0.1 M. The voltammetric measurements were performed using a platinum-disk electrode (*d* = 2 mm), which was polished prior to use. Potentials were calibrated by the method of Gagné and are quoted versus the ferrocenium-ferrocene couple as internal standard.<sup>[22]</sup> A platinum wire was used as a counter electrode.

**Starting materials:** 1,1'-Bis(dimethylgallyl)ferrocene (**1**)<sup>[5]</sup> and the digalla-[1.1]ferrocenophane **2**<sup>[3b]</sup> were prepared by using literature procedures.

**Preparation of 3:** Method a: Compound **1** (200 mg, 0.52 mmol) or **2** (200 mg, 0.37 mmol) was mixed with *p*-xylene (3 mL) in a Schlenk flask. In the tightly closed flask, the suspension was heated for 15 min to 150 °C. After the mixture was cooled to room temperature and the supernatant solvent was decanted, the residue was washed with hexane and dried in vacuo to give **3** (80 mg, 0.12 mmol; 69%) as an orange solid. Method b: Compound **1** (200 mg, 0.52 mmol) or **2** (200 mg, 0.37 mmol) was heated in vacuo for 2 h to 200 °C without melting. The resulting solid was washed with *n*-hexane to remove impurities, resulting from thermal decomposition. The residue was dried in vacuo to give **3** (50 mg, 0.07 mmol; 40%) as an orange solid. Method c: In a Schlenk flask **1** (200 mg, 0.29 mmol) was treated with diethyl ether (1 mL) and toluene (3 mL) at room temperature. The reaction mixture was heated for 5 min to 130 °C and then cooled to +6 °C. After one day an orange, crystalline solid had formed, which was washed with *n*-hexane and dried in vacuo to give **3** (55 mg, 0.08 mmol; 43%) as an orange powder.



**3:**  $^1\text{H NMR}$  ( $[\text{D}_6]\text{DMSO}$ ):  $\delta = 4.20$  (s, 12H; ring-C2/5-H or -C3/4-H), 4.30 ppm (s, 12H; ring-C2/5-H or -C3/4-H);  $^{13}\text{C NMR}$  ( $[\text{D}_6]\text{DMSO}$ ):  $\delta = 69.2$  (ring-C2/5 or -C3/4), 74.9 ppm (ring-C2/5-H or -C3/4-H); MS:  $m/z$  (%): 692 (3) [ $M^+$ ]; elemental analysis calcd (%) for  $\text{C}_{30}\text{H}_{24}\text{Fe}_3\text{Ga}_2$  ( $M = 691.51 \text{ g mol}^{-1}$ ): C 52.11, H 3.50; found: C 51.79, H 3.51.

**Preparation of 3a-d:** Method a: In a Schlenk flask, **1** (300 mg, 0.78 mmol), or **2** (210 mg, 0.39 mmol), or **3** (180 mg, 0.26 mmol) were treated with toluene (3 mL) and the respective donor (1 mmol). In the tightly closed flask, the reaction mixture was heated to 130°C for 5 min. After the mixture was cooled to room temperature, a crystalline solid formed over a few days. The solid was washed with *n*-hexane and dried in vacuo. Yields are given for this method. Method b: In a Schlenk flask, **2a** or **2b** (0.4 mmol) were treated with toluene (3 mL). The reaction mixture was heated to 130°C for 5 min in the tightly closed flask. After the mixture was cooled to room temperature, a crystalline solid formed over a few days. The solid was washed with *n*-hexane and dried in vacuo to give **3a** or **3b**, respectively.

Crystals of **3b** and **3c** contain cocrystallized solvent molecules. When they were dried in vacuo solvent was removed and the crystals decomposed to an amorphous solid.

**3a:**  $^1\text{H NMR}$  ( $[\text{D}_6]\text{DMSO}$ ):  $\delta = 1.08$  (t,  $^3J(\text{H,H}) = 6.9 \text{ Hz}$ , 12H;  $\text{Et}_2\text{O}$ ), 3.37, (q,  $^3J(\text{H,H}) = 6.9 \text{ Hz}$ , 8H;  $\text{Et}_2\text{O}$ ), 4.20 (s, 12H; ring-C2/5-H or -C3/4-H), 4.30 ppm (s, 12H; ring-C2/5-H or -C3/4-H);  $^{13}\text{C NMR}$  ( $[\text{D}_6]\text{DMSO}$ ):  $\delta = 15.1$  ( $\text{Et}_2\text{O}$ ), 64.9, ( $\text{Et}_2\text{O}$ ), 69.2 (ring-C2/5 or -C3/4), 74.9 ppm (ring-C2/5 or -C3/4); **3a** is thermolabile and decomposes already at room temperature.<sup>[23]</sup>

**3b:** Yield 76 mg (0.11 mmol, 42%) **3b.**  $^1\text{H NMR}$  ( $[\text{D}_6]\text{DMSO}$ ):  $\delta = 4.20$  (s, 12H; ring-C2/5-H or -C3/4-H), 4.30 (s, 12H; ring-C2/5-H or -C3/4-H), 7.38 (s, 4H; pyridine), 7.78 (s, 2H; pyridine), 8.55 ppm (s, 4H; pyridine);  $^{13}\text{C NMR}$  ( $[\text{D}_6]\text{DMSO}$ ):  $\delta = 69.2$  (ring-C2/5 or -C3/4), 74.9 (ring-C2/5 or -C3/4), 123.9 (pyridine), 125.3 (pyridine), 150.3 ppm (pyridine); MS:  $m/z$  (%): 692 (22) [ $M^+ - 2$  pyridine], 79 (100) [pyridine $^+$ ]; elemental analysis calcd (%) for  $\text{C}_{40}\text{H}_{34}\text{Fe}_3\text{Ga}_2\text{N}_2$  ( $M = 849.71 \text{ g mol}^{-1}$ ): C 56.54, H 4.03, N 3.30; found: C 56.17, H 3.93, N 3.27; CV:  $E_{1/2}(1) = -356 \text{ mV}$ ,  $E_{1/2}(2) = -154 \text{ mV}$ ,  $E_{1/2}(3) = 8 \text{ mV}$  (peak separation 90 mV).

**3c:** Yield 85 mg (0.10 mmol, 38%) **3c.**  $^1\text{H NMR}$  ( $[\text{D}_6]\text{DMSO}$ ):  $\delta = 2.49$  (s, 12H; DMSO), 4.20 (s, 12H; ring-C2/5-H or -C3/4-H), 4.30 ppm (s, 12H; ring-C2/5-H or -C3/4-H);  $^{13}\text{C NMR}$  ( $[\text{D}_6]\text{DMSO}$ ):  $\delta = 39.5$  ( $\text{CH}_3$  in DMSO), 69.2 (ring-C2/5 or -C3/4), 74.9 ppm (ring-C2/5 or -C3/4); MS:  $m/z$  (%): 692 (1) [ $M^+ - 2$  DMSO], 78 (2) [DMSO $^+$ ]; elemental analysis was not successful due to tenacious retainment of fractional amounts of solvent.

**3d:** Yield 137 mg (0.17 mmol, 64%) **3d.**  $^1\text{H NMR}$  ( $[\text{D}_6]\text{DMSO}$ ):  $\delta = 4.20$  (s, 12H; ring-C2/5-H or -C3/4-H), 4.30 (s, 12H; ring-C2/5-H or -C3/4-H), 8.66 ppm (s, 4H; pyrazine).  $^{13}\text{C NMR}$  ( $[\text{D}_6]\text{DMSO}$ ):  $\delta = 69.2$  (ring-C2/5 or -C3/4), 74.9 (ring-C2/5 or -C3/4), 145.2 ppm (pyrazine). MS:  $m/z$  (%): 692 (2) [ $M^+ - \text{pyrazine}$ ], 80 (4) [pyrazine $^+$ ]; elemental analysis was not successful due to tenacious retainment of fractional amounts of solvent.

**Reaction of 3 and 3a-c with trimethylgallium:** Method a: Trimethylgallium ((pyrophoric!)) 100 mg, 0.9 mmol) was added to a suspension of **3** (30 mg, 43  $\mu\text{mol}$ ) in  $[\text{D}_8]\text{toluene}$  (0.5 mL) in a NMR tube. The reaction mixture was heated to 100°C in the tightly closed tube until all components had dissolved. On cooling the mixture to room temperature, **1** formed as an orange microcrystalline solid. The supernatant solution was decanted, and the solid residue was washed with hexane, and identified by using NMR spectroscopy. Method b: Trimethylgallium ((pyrophoric!)) 50 mg, 0.45 mmol) was added to a suspension of **3** (30 mg, 43  $\mu\text{mol}$ ) in  $[\text{D}_8]\text{toluene}$  (0.5 mL) in a NMR tube. The reaction mixture was heated to 100°C in the tightly closed tube until all components had dissolved. On cooling the mixture to room temperature, **2** formed as an orange microcrystalline solid. The supernatant solution was decanted, and the solid residue was washed with hexane, and identified by using NMR spectroscopy. Only  $\text{GaMe}_3$  could be identified in the reaction mixture by NMR spectroscopy.

The coordination compounds **3a-c** react with trimethylgallium in a similar manner. The donor adduct of  $\text{GaMe}_3$  and uncoordinated  $\text{GaMe}_3$  were identified in the reaction mixture.

## Acknowledgement

The support of this work by the Deutsche Forschungsgemeinschaft, the Universität Bielefeld and the Fonds der Chemischen Industrie is gratefully acknowledged. We thank Professor Lorberth, University of Marburg for a gift of trimethylgallium.

- [1] For metal-metal interactions in linked metallocenes see: S. Barlow, D. O'Hare *Chem. Rev.* **1997**, *97*, 637–669.
- [2] Review on [*m,m*]ferrocenophanes: U. T. Mueller-Westerhoff, *Angew. Chem.* **1986**, *98*, 700; *Angew. Chem. Int. Ed. Engl.* **1986**, *25*, 702–717.
- [3] a) M. Scheibitz, R. F. Winter, M. Bolte, H.-W. Lerner, M. Wagner, *Angew. Chem.* **2003**, *115*, 954; b) A. Althoff, P. Jutzi, N. Lenze, B. Neumann, A. Stammer, H.-G. Stammer, *Organometallics* **2003**, *22*, 2766–2774; c) W. Uhl, I. Hahn, A. Jantschak, T. Spies, *J. Organomet. Chem.* **2001**, *637–639*, 300–303; d) D. L. Zechel, D. A. Foucher, J. K. Pudelski, G. P. A. Yap, A. L. Rheingold, I. Manners, *J. Chem. Soc. Dalton Trans.* **1995**, 1893–1899; e) A. Clearfield, C. J. Simmons, H. P. Withers, D. Seyferth, *Inorg. Chim. Acta* **1983**, *75*, 139–144; f) G. Utri, K.-E. Schwarzans, G. M. Z. Allmaier, *Z. Naturforsch. B* **1990**, *45*, 755–762.
- [4] T. Katz, W. Slusarek, *J. Am. Chem. Soc.* **1980**, *102*, 1058–1063.
- [5] A. Althoff, P. Jutzi, N. Lenze, B. Neumann, A. Stammer, H.-G. Stammer, *Organometallics* **2002**, *21*, 3018–3022.
- [6] Software used: Gaussian98 (Revision A.7), M. J. Frisch, G. W. Trucks, H. B. Schlegel, G. E. Scuseria, M. A. Robb, J. R. Cheeseman, V. G. Zakrzewski, J. A. Montgomery, R. E. Stratmann, J. C. Burant, S. Dapprich, J. M. Millam, A. D. Daniels, K. N. Kudin, M. C. Strain, O. Farkas, J. Tomasi, V. Barone, M. Cossi, R. Cammi, B. Mennucci, C. Pomelli, C. Adamo, S. Clifford, J. Ochterski, G. A. Petersson, P. Y. Ayala, Q. Cui, K. Morokuma, D. K. Malick, A. D. Rabuck, K. Raghavachari, J. B. Foresman, J. Cioslowski, J. V. Ortiz, B. B. Stefanov, G. Liu, A. Liashenko, P. Piskorz, I. Komaromi, R. Gomperts, R. L. Martin, D. J. Fox, T. Keith, M. A. Al-Laham, C. Y. Peng, A. Nanayakkara, C. Gonzalez, M. Challacombe, P. M. W. Gill, B. G. Johnson, W. Chen, M. W. Wong, J. L. Andres, M. Head-Gordon, E. S. Replogle, J. A. Pople, Gaussian, Inc., Pittsburgh, PA, **1998**.
- [7] G. H. Robinson, *Acc. Chem. Res.* **1999**, *32*, 773–782.
- [8] Software used: NBO Version 3.1, A. E. Reed, L. A. Curtiss, F. Weinhold, *Chem. Rev.* **1988**, *88*, 899–926.
- [9] A. D. Becke, K. E. Edgecombe, *J. Chem. Phys.* **1990**, *92*, 5397–5403.
- [10] The formation of a B–B one-electron sigma-bond on reduction of diborylated naphthalene has been described: J. D. Hoefelmeyer, F. P. Gabbai, *J. Am. Chem. Soc.* **2000**, *122*, 9054–9055.
- [11] We have reported about this compound in a preliminary communication: P. Jutzi, N. Lenze, B. Neumann, H.-G. Stammer, *Angew. Chem.* **2001**, *113*, 1470–1473; *Angew. Chem. Int. Ed.* **2001**, *40*, 1424–1427.
- [12] G. E. Coates, *J. Chem. Soc.* **1951**, 2003–2013.
- [13] S. C. Jones, S. Barlow, D. O'Hare, *Chem. Eur. J.* **2005**, *11*, 4473–4481.
- [14] Spectroelectrochemical studies performed by Prof. Dr. M. D. Ward, University of Sheffield.
- [15] Software used: TURBOMOLE, Programm Package for ab initio Electronic Structure Calculations, Version 5.7: a) R. Ahlrichs, M. Bär, M. Häser, H. Horn, C. Kölmel, *Chem. Phys. Lett.* **1989**, *163*, 165–169; b) A. Schäfer, H. Horn, R. Ahlrichs, *J. Chem. Phys.* **1992**, *97*, 2571–2577; c) K. Eichkorn, O. Treutler, H. Öhm, M. Häser, R. Ahlrichs, *Chem. Phys. Lett.* **1995**, *242*, 652–660; d) K. Eichkorn, F. Weigend, O. Treutler, R. Ahlrichs, *Theor. Chem. Acc.* **1997**, *97*, 119–124.
- [16] Detailed DFT calculations on a ferrocenylborane condensation reaction with a H atom in a bridging position have been described in: J. B. Heilmann, M. Scheibitz, Y. Qin, A. Sundararaman, F. Jäkle, T. Kretz, M. Bolte, H.-W. Lerner, M. C. Holthausen, M. Wagner, *Angew. Chem.* **2006**, *118*, 934–939; *Angew. Chem. Int. Ed.* **2006**, *45*, 920.

- [17] Review on dynamic covalent chemistry: S. J. Rowan, S. J. Cantrill, G. R. L. Cousins, J. K. M. Sanders, J. F. Stoddart, *Angew. Chem.* **2002**, *114*, 938–993; *Angew. Chem. Int. Ed.* **2002**, *41*, 898–952.
- [18] F. P. Gabbai, A. Schier, J. Riede, *Angew. Chem.* **2003**, *115*, 2318–2321; *Angew. Chem. Int. Ed.* **2003**, *42*, 2218–2221.
- [19] J. F. Blount, P. Finocchiaro, D. Gust, K. Mislow, *J. Am. Chem. Soc.* **1973**, *95*, 7019–7029.
- [20] P. Jutzi, D. Meyer, unpublished results.
- [21] a) Artificial molecular machines: V. Balzani, A. Credi, F. M. Raymo, J. E. Stoddart, *Angew. Chem.* **2000**, *112*, 3484–3530; *Angew. Chem. Int. Ed.* **2000**, *39*, 3348–3391; b) artificial molecular rotors: G. S. Kottas, L. I. Clarke, D. Horinek, J. Michl, *Chem. Rev.* **2005**, *105*, 1281–1376.
- [22] R. R. Gagné, C. A. Koval, G. C. Lisensky, *Inorg. Chem.* **1980**, *19*, 2854–2855.
- [23] A single crystal was coated with a layer of hydrocarbon oil, attached to a glass fiber, and cooled to 173 K for an X-ray structure determination. Because of the thermolability of **3a** no elemental analysis could be performed.

Received: February 16, 2006  
 Published online: May 8, 2006